BIAXIAL FATIGUE DESIGN PROCEDURE APPLIED TO WELDED PLATE STRUCTURES

G. J. Moyar* and V. K. Garg**

**Moyar Technical Services, Inc., 2051 Ogden Ave., Suite D, Downers Grove, IL 60515, USA*
***Department of Mechanical Engineering, University of Maine, Orono, ME 04473, USA*

ABSTRACT

Several biaxial fatigue theories are evaluated and the concept of fatigue equivalent uniaxial stress is applied. The approach is illustrated in a practical welded beam example, using previously published fatigue data. These fatigue data were obtained from test beams with different web reinforcement details.

The derivation of the fatigue equivalent uniaxial stress cycle based on the modified maximum range of shear theory provides a conservative design tool that has been demonstrated to satisfactorily correlate fatigue data from different regions of a welded beam. It is recommended for use in nominal stress design approaches as a practical means of making short-range extrapolations from existing data.

KEYWORDS

Fatigue; equivalent uniaxial stress cycle; welded beam; test data; range of shear stress; principal stress.

INTRODUCTION

A number of theories and design guidelines have evolved over the years for the treatment of fatigue resulting from multiaxial loading [1-5], yet the great bulk of data is still for uniaxial loading. These guidelines range from simple nominal stress methods to more elaborate cyclic local strain methods with associated nonlinear stress analyses [6,7]. The practical designer, however is still largely dependent on uniaxial nominal stress concepts and the related body of stress data (σ-N curves and Modified Goodman Diagrams) for many typical fabricated structural details. The current design guidelines [8] for the fatigue analysis of freight car structures in North American interchange railroad service describe such an approach.

In the fatigue design evaluation of conventional welded steel structural com-

ponents, the designer tries to make use of fatigue "properties" which are derived from tests of structural weldments, subjected primarily to bending or axial loads. However, in most applications the loading is multiaxial. Furthermore, even with single loading on a component, the state of nominal stress can be biaxial in the fatigue critical locations.

To handle this problem rationally and to use the conventional fatigue data base, the concept of fatigue equivalent uniaxial stress is used and several biaxial fatigue theories are evaluated. The approach is illustrated in a practical welded beam example, using previously published fatigue data [9,10] which were obtained from test beams with different web reinforcement details. The existing fatigue data are extrapolated from one region of a beam to another, where the state of nominal stress is different, although the local stress concentration and weld details are similar. Furthermore, the study is restricted to in-phase loading, since stress biaxiality arises in this case from a single load source. It is hoped that this modest data correlation exercise will provide the designer with a demonstrated guideline for solving the more general problem of structures subjected to externally applied combined loading.

FATIGUE EQUIVALENT UNIAXIAL STRESS

A designer often uses a Modified Goodman Diagram to determine the fatigue limit for a specific design detail and stress ratio R ($=\sigma_{min}/\sigma_{max}$) under a uniaxial stress state. This fatigue limit denotes the maximum stress, σ_{max}, which may be applied to the detail for an infinite number of times at that stress ratio, without producing a fatigue failure. The application of maximum stresses of any larger magnitude, if applied often enough, would eventually result in a fatigue failure of the part:

$$\sigma_{max} = b + m\,\sigma_{min} \tag{1}$$

where b is the fatigue limit at $R = 0$ and m is the slope of the Goodman line.

On expressing Eq. (1) in terms of alternating stress, $\sigma_a[=(\sigma_{max}-\sigma_{min})/2]$ and mean stress, $\sigma_m[=(\sigma_{max}+\sigma_{min})/2]$, one gets:

$$b/(1+m) = \sigma_a + [(1-m)/(1+m)]\sigma_m = \sigma_{eq} \tag{2}$$

where σ_{eq} is the amplitude of the fatigue equivalent uniaxial stress for completely reversed loading.

The fatigue strength of a component subjected to combined stresses is investigated by expressing several fatigue failure criteria in terms of σ_{eq} and m. Fatigue failure criteria for combined stresses are based on physical concepts of failure, similar to those used for static combined stresses, i.e., fatigue failure under combined stresses is envisioned when a limiting normal stress, shear stress or energy is reached which corresponds to the values at failure under uniaxial fluctuating stress. In this study the following fatigue failure criteria are investigated:

1. Maximum Principal Stress [11]: The principal stresses vary so that their maximum values are σ_1 and σ_2, respectively. The maximum principal stress theory considers only the variation of the largest principal stress. Thus, for the biaxial stress state, in which the largest principal stress varies from 0 to σ_1, Eq. (2) becomes:

$$\sigma'_{eq} = \sigma_1/2 + [(1-m)/(1+m)](\sigma_1/2) \tag{3}$$

2. Modified Maximum Range of Shear Stress [1]: This theory assumes that the allowable amplitude of shear stress, τ_a, on the plane of maximum shear stress range is equal to the fatigue equivalent amplitude of shear stress τ_{eq}, (on a plane for which the average normal stress is zero) minus an influence factor, k, times the average value of the normal stress, σ_{na}, on the plane:

$$\tau_a = \tau_{eq} - k\,\sigma_{na} \tag{4}$$

For the biaxial stress state, in which the maximum shear plane is perpendicular to the plate surface and the loading varies from zero to peak, Eq. (4) can be written as:

$$\tau_{eq} = (\sigma_1-\sigma_2)/4 + k\ \ (\sigma_1+\sigma_2)/4 \tag{5}$$

Eq. (5) can be rewritten in the same form as Eq. (2) by multiplying Eq. (5) by two and using $k = (1-m)/(1+m)$.

$$\sigma''_{eq} = 2\tau_{eq} = (\sigma_1-\sigma_2)/2 + [(1-m)/(1+m)]\ (\sigma_1+\sigma_2)/2 \tag{6}$$

3. Maximum Octahedral Shear Stress [12]: This method uses the alternating octahedral shear stress, and for biaxial stresses can be expressed as:

$$\sigma'''_{eq} = \tfrac{1}{2}(\sigma^2_{a1} - \sigma_{a1}\sigma_{a2}+\sigma^2_{a2})^{\frac{1}{2}} + \rho(\sigma_{m1}+\sigma_{m2})/2\sqrt{2} \tag{7}$$

where σ_{ai} = alternating component of the principal nominal stress, σ_{mi} = mean component of the principal nominal stress, ρ = coefficient of mean stress influence, σ'''_{eq} = amplitude of the fatigue equivalent uniaxial stress for completely reversed loading.

By denoting ρ in terms of m as $\rho = \sqrt{2}\ (1-m)/(1+m)$ and using $\sigma_{ai} = \sigma_i/2$ and $\sigma_{mi} = \sigma_i/2$ for the zero to peak loading, Eq. (7) can be rewritten as:

$$\sigma'''_{eq} = 0.5(\sigma^2_1-\sigma_1\sigma_2+\sigma^2_2)^{\frac{1}{2}} + [(1-m)/(1+m)]\ (\sigma_1+\sigma_2)/2 \tag{8}$$

It can be observed that the condition for $m=1$ in Eqs. (3), (6) and (8) refers to the situation where the effect of mean stress is ignored. For a number of steel weldments this is a good approximation as recommended by Fisher [13]. Generally, however, m will be a function of the number of cycles to failure. The dependence on mean stress at low to moderate stress levels (or long lives) is, nevertheless, slight as demonstrated by the success of the Gerber parabola [12] in fitting fatigue data in the region of low mean stress.

TEST DATA

The data used in the analysis were obtained from tests conducted at the University of Illinois and reported earlier [9,10]. The dimensions of the mild steel fabricated beam specimens, location of stiffners, and points of application for loads are given in Fig. 1. The weld details are shown in Fig. 2. Type B refers to continuous 3/16 in. welds, whereas Type C refers to noncontinuous or intermittent 3/16 in. welds. The loads were applied in such a way as to subject the flanges of the specimen to cycles of flexural stress.

Table 1 gives a summary of the test results and the values of the principal stresses computed at the point of initiation of the crack, based on data from Munse [14].

ANALYSIS OF DATA

The fatigue equivalent uniaxial stresses were calculated using the three fatigue failure criteria mentioned previously. These values of the fatigue equivalent uniaxial stresses for $m = 1$ have been plotted against the number of cycles for failure recorded during the tests, in Figs. 3, 4 and 5. The

least squares best fit straight line is drawn through the individual data sets. In deriving this "best fit", the data point corresponding to failure in the compression web was ignored. As may be observed from a comparison of Figs. 3, 4 and 5, the maximum range of shear theory appears to do the best job of bringing the fatigue results of both B and C beam types into coincidence.

Another method of checking the ability of various theories to correlate fatigue data from different biaxial stress states is to derive the fatigue properties based on one set of data and then predict the cycles to failure for individual tests from the other set. For this purpose the data for the Type C beams, for which there are more tests, were used to obtain the fatigue properties, b and k used in conventional stress-life equation

$$N = N_e \, (\sigma_e/\sigma)^{1/k} \tag{9}$$

where N_e is the endurance limit, usually taken as 2,000,000 cycles, σ_e is the fatigue limit or stress which produces failure in N_e cycles, k is the absolute value of the slope of the log σ - log N diagram.

The fatigue limit may be expressed in terms of the limit for 0 to tension cycling, b, the stress ratio, R, and the slope of the Modified Goodman Diagram as:

$$\sigma_e = b/(1-mR) \tag{10}$$

From Type C data on the σ-N diagrams of Figs. 3, 4 and 5, the fatigue properties k and σ_e or b (fatigue strength at 2,000,000 cycles) were obtained from a least squares linear regression analysis and tabulated below for the three fatigue theories.

Theory	σe	k
Maximum Principal Stress	18.60	0.19
Modified Max. Range Shear Stress	28.20	0.22
Maximum Octahedral Shear Stress	24.86	0.22

A comparison of the corresponding predictions for the three theories versus the observed cycles to failure for the type B beam specimens is provided in Table 2. The mean and standard deviation of the difference of predicted minus observed cycles to failure were calculated and included in this table. Again, the maximum shear range theory appears more satisfactory in that the mean difference in prediction and observation is smaller. Overall, the maximum principal stress theory is the least conservative; that is, it predicts longer lives than observed.

GENERALIZATION

In order to gain a better understanding of the mean stress effect and performance of the fatigue criteria in general for beam type structures, the fatigue equivalent uniaxial stresses from Eqs. (3), (6) and (8) are expressed in terms of nominal bending and shear stresses at the web failure location.

Since $$\sigma_1 = (\sigma/2)\,(1+\sqrt{1+\eta^2}) \tag{11}$$

and $$\sigma_2 = (\sigma/2)\,(1-\sqrt{1+\eta^2}) \tag{12}$$

where σ = nominal bending stress at the failure location and $\eta = 2\tau/\sigma$, τ = nominal shear stress at failure location. On substituting Eqs. (11) and (12) into Eqs. (3), (6) and (8), one gets

$$2(\sigma'_{eq}/\sigma) = (1+\sqrt{1+\eta^2})/(1+m) \tag{13}$$

$$2(\sigma''_{eq}/\sigma) = \sqrt{1+\eta^2} + (1-m)/(1+m) \tag{14}$$

$$2(\sigma'''_{eq}/\sigma) = \sqrt{1+0.75\eta^2} + (1-m)/(1+m) \tag{15}$$

These equations have been plotted in Fig. 6 to show the relationships between normalized fatigue equivalent uniaxial stress and normalized shear stress for $m = 1.0$. Fig. 6 is convenient for design purposes to obtain the fatigue equivalent uniaxial stress for any location in the beam when the nominal bending and shear stress are known at that location. It may be seen in Fig. 6 that the maximum principal stress theory becomes increasingly unconservative as the amount of shear in the biaxial state increases.

DISCUSSION

In the original presentation of these fatigue data Munse [10] noted that all the test beams had about the same total flexural resistance. However, he observed that the web failures initiated at locations where the flexural stress was considerably below the maximum. He also observed that the cracks seemed to propagate in a direction perpendicular to the maximum principal tensile stress and, therefore, concluded that the maximum principal tensile stress or normal stress at the failure location would correlate the data better than the maximum flexural stress at the failure section.

While it is true as Munse stated that "one should take into account the effect of shear upon the principal tensile stress in the web of the member" [10], it is believed that the modified range of shear or octahedral shear theory is more suitable for conservative prediction of fatigue initiation than the maximum principal stress theory.

CONCLUSION

The derivation of the fatigue equivalent uniaxial stress cycle based on the modified maximum range of shear theory provides a conservative design tool that has been demonstrated to satisfactorily correlate fatigue data from different regions of a weld fabricated beam. It is recommended for use in nominal stress design approaches, not as a fundamental new theory, but as a practical means of making short range extrapolations from existing data for fatigue crack initiation in representative weldment details.

This approach takes into account the important nominal biaxial stress range differences that may exist from one fatigue-critical location to another. However, its implementation still depends on crack initiation data from conventional tests with similar weldment details and materials wherein the local stress concentrations are basically equivalent. It is not offered as an alternate or replacement method for the more advanced crack initiation prediction techniques. The advanced techniques are dependent on calculated or measured local strains and are used to extrapolate fundamental fatigue properties to new structural configurations.

The success of a biaxial fatigue theory based on the maximum range of shear stress in correlating fatigue crack initiation data should not be surprising in view of much fundamental research relating the plastic slip mechanisms of fatigue crack initiation to the critical range of reversed shear. However, analysis of the stages of fatigue involving crack propagation would require additional fracture mechanics consideration that is beyond the scope of this paper.

ACKNOWLEDGEMENTS

William H. Munse, Professor (emeritus) of Civil Engineering of the University of Illinois, has kindly provided us with much additional information regarding his previously published work on which our demonstration of data correlation depends. We offer him our sincere thanks while taking responsibility for any errors or misinterpretations that may be found in our analysis of his experiments.

We also express our appreciation to the Association of American Railroads, especially Mr. Keith Hawthorne, Mr. James Lundgren, Mr. Roy Allen and Dr. Roger Steele.

REFERENCES:

1. Little, R.E., and R. W. Little (1965), "Analysis of Two Dimensional Cyclic Stress", Ninth Midwestern Mechanics Conference, Madison, Wis.
2. Mitchell, L. D., and D. T. Vaughn (1974), "A General Method for the Fatigue-Resistant Design of Mechanical Components, Part I, Graphical; Part II, Analytical", ASME Papers 74-WA/DE-4 and 75-WA/DE-5.
3. Kececioglu, Dimitri, Louie B. Chester, and Thomas M. Dodge (1974), "Combined Bending-Torsion Fatigue Reliability of AISI 4340 Steel Shafting with kt = 2.34", ASME Paper 74-WA/DE12.
4. Miller, W.R., K. Ohji, and J. Marin (1967), "Rotating Principal Stress Axes in High-Cycle Fatigue", ASME Journal of Basic Engineering, 3, pp. 76-80.
5. Marin, J. (1965), "Interpretation of Fatigue Strengths for Combined Stress", International Conference on Fatigue of Metals, London, England.
6. Socie, D. F. (1977), "Fatigue Life Prediction Using Local Stress-Strain Concepts", Experimental Mechanics, SESA, 2, pp. 50-56.
7. Kelley, F. S. (1980), "A General Fatigue Evaluation Method", ASME Journal of Pressure Vessel Technology, Vol. 102, pp. 287-293.7.
8. AAR (1979), "Fatigue Analysis Methods", Manual of Standards and Recommended Practices, Section C - Part II, Volume I, M-1001.
9. Wilson, W. M. (1948), "Flexural Fatigue Strength of Steel Beams", University of Illinois Bulletin, No. 33, Vol. 45, Urbana, Illinois.
10. Munse, W. H. (1964), "Fatigue of Welded Steel Structures", Editor La Motte Grover, Welding Research Council, New York, N.Y.
11. Marin, J. (1962), Mechanical Behavior of Engineering Materials, Prentice - Hall, Inc., Englewood Cliffs, N.J.
12. Fuchs, H. O. and R. I. Stephans (1980), Metal Fatigue in Engineering, John Wiley, New York, N.Y.
13. Fisher, J. W. and T. T. Yen (1979), "Minimizing Fatigue and Fracture in Steel Bridges", ASME Structural Integrity Technology, p. 155.
14. Munse, W. H. (1980), Private correspondence to G. J. Moyar.

TABLE 1 Summary of Test Results

Specimen #(AA-)	Maximum Flexural Stress (ksi)	Cycles to Failure (millions)	Primary Fracture Location Stiffener ***	Principal Stress at Pt. of Crack Initiation (ksi) Max.	Min.
TYPE B:					
29(0)B*+SB**	31.4	0.6278	2	30.71	-9.77
30(0)B+SB	31.1	0.4467	1	34.89	-8.45
31(0)B+SB	31.0	0.5236	1	34.76	-8.42
41(0)B+SB	25.3	1.1103	2	24.76	-7.89
43(0)B+SB	25.8	1.2719	2	22.08	-9.18
TYPE C:					
13(0)A+SC	29.5	0.9113	5	22.3	-12.54
14(0)A+SC	30.0	0.6493	3	26.2	-11.03
15(0)A+SC	29.9	0.8642	5	22.6	-12.72
44(0)B+SC	24.5	1.9025	4	17.42	-11.07
45(0)B+SC]	24.9	1.7527	4	17.71	-11.25
46(0)B+SC	25.3	1.0487	4	17.99	-11.43
57(0)B+SC	20.0	2.8323	2	17.65	-7.28
58(0)B+SC	19.7	4.6082	2	17.39	-7.18

NOTES:
* B or A in this position of specimen identification code refers to beam welding sequence. See Figs. 1a or 1b.
** B or C in this position of specimen identification code refers to stiffener type. See Fig. 2.
*** Number refers to stiffener location. See Figs. 1a or 1b.

TABLE 2 Comparison of Predicted Cycles to Failure (in Millions) of Type B Beams Using Properties from Type C Beam Data and Biaxial Fatigue Theories

SPEC. # AA-SC	OBS. CYCLES TO FAIL.	MAX. PRIN. STRESS THEORY PREDICT.	DIFF.	MAX. SHEAR STRESS THEORY PREDICT.	DIFF.	MAX. OCT. STRESS THEORY PREDICT.	DIFF.
29(0)B	0.6278	0.1426	-0.4852	0.3868	-0.2410	0.3456	-0.2822
30(0)B	0.4467	0.0731	-0.3736	0.2836	-0.1631	0.2355	-0.2112
31(0)B	0.5236	0.0744	-0.4492	0.2884	-0.2352	0.2399	-0.2837
41(0)B	1.1103	0.4438	-0.6665	1.0261	-0.0842	0.9188	-0.1915
43(0)B	1.2719	0.8111	-0.4608	1.2522	-0.0197	1.1994	-0.0725
		MEAN	-0.4871		-0.1486		-0.2082
		STD. DEV.	0.1086		0.0962		0.0864

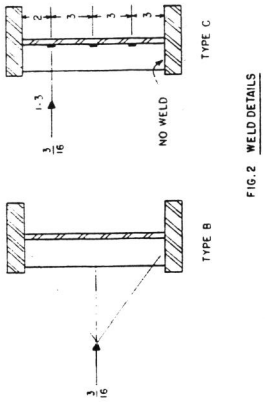

FIG. 2 WELD DETAILS

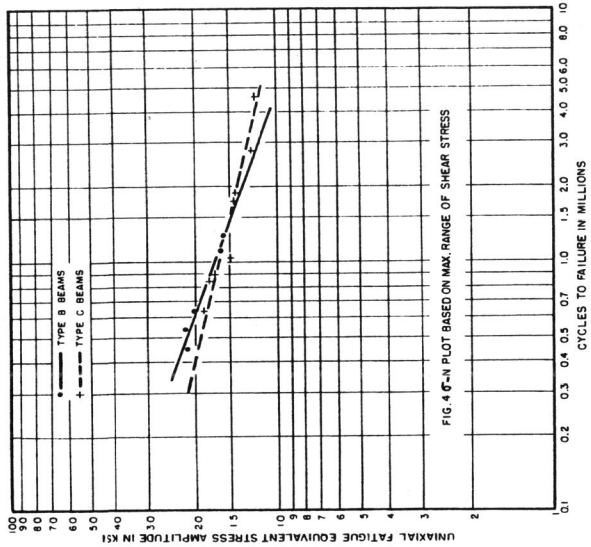

FIG. 4 σ-N PLOT BASED ON MAX. RANGE OF SHEAR STRESS

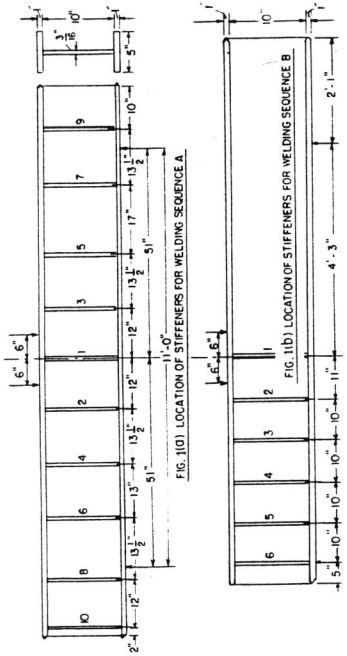

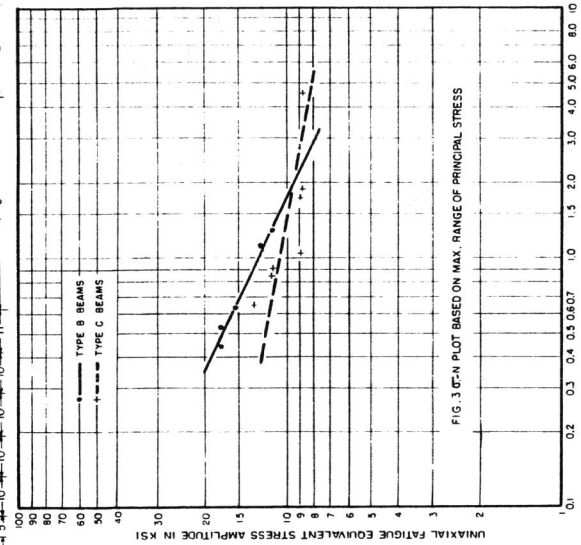

FIG. 3 σ-N PLOT BASED ON MAX. RANGE OF PRINCIPAL STRESS

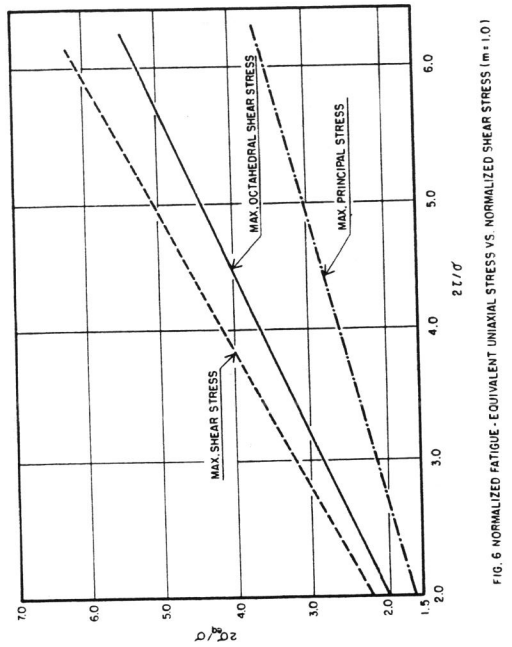

FIG. 6 NORMALIZED FATIGUE - EQUIVALENT UNIAXIAL STRESS VS. NORMALIZED SHEAR STRESS (m = 1.0)

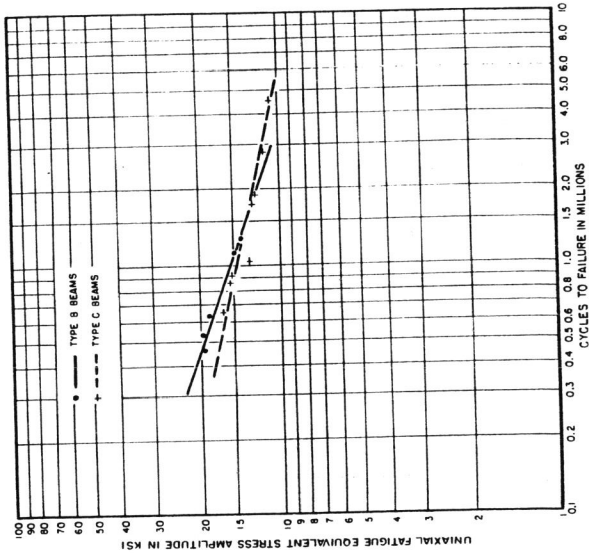

FIG. 5 σ-N PLOT BASED ON MAX. RANGE OF OCTAHEDRAL SHEAR